Kinetics of Gas-Phase Ethylene Polymerization with Morphology-Controlled $MgCl_2$-Supported $TiCl_4$ Catalyst

L. Wu, D. T. Lynch, and S. E. Wanke*

Department of Chemical and Materials Engineering, University of Alberta, Edmonton, Alberta, Canada T6G 2G6

Received May 28, 1999; Revised Manuscript Received September 27, 1999

ABSTRACT: A new method is proposed to determine the power-law order of gas-phase ethylene homopolymerization rate with time-varying activities over morphology-controlled prepolymerized catalyst at temperatures of 30−70 °C and ethylene concentrations of 120−900 mol/m^3. The prepolymerized catalyst was obtained by ethylene prepolymerization at mild conditions in heptane using a catalyst, in which $TiCl_4$ was supported on spherical $MgCl_2$ prepared by melt quenching of the $MgCl_2$−ethanol complex. Triethylaluminum was used as a cocatalyst for prepolymerization and homopolymerization. During ethylene homopolymerization, the overall rate changed markedly with time, and two maxima in activity were observed in the absence of mass transfer effects. The order of power-law rate functions with respect to ethylene concentration was not constant and decreased with time on stream from about 1.5 to about 1.0 after about 4 h. These results show the presence of at least two types of catalytic sites having rates with different ethylene concentration dependencies and suggest that the two different types of catalytic sites have different deactivation behavior in this heterogeneous Ziegler−Natta catalyst.

Introduction

It is well-known that one of the important features of the heterogeneous Ziegler−Natta polymerization is the capability of these catalysts to replicate their morphology into the morphology of polymer granules.[1] This suggests that the control of catalyst particle morphology is the key to the control and modification of polymer morphology. Morphology-controlled polyolefins made directly in reactors (so-called reactor polyolefin granules) are polyolefin granules that have spherical shape, high bulk density, high flowability, and large size with narrow particle size distribution and low content of fines. Reactor polyolefin granules have advantages in terms of energy saving in polymerization processes and product processing.[2] Commercial production of reactor polyolefin granules is frequently carried out in multistage processes in which the reactors are arranged in series, for example, the SPHERIPOL and SPHERILENE processes developed by Himont Inc.[3,4] To achieve proper performances of catalysts in terms of morphology and activity, a small amount of polymerization, called prepolymerization, is carried out in the first reactor operated in the slurry mode under mild conditions at low temperature and low monomer pressure. The majority of the polymerization is done in the subsequent gas-phase reactor.

The kinetics of Ziegler−Natta polymerization has been one of the most controversial areas ever since Ziegler's discovery because Ziegler−Natta catalysts are very sensitive to impurities that cause catalytic deactivation and frequently prevent the collection of unequivocal kinetic data. For supported Ziegler−Natta catalytic polymerization of olefins, polymerization rates have been observed to change with time under polymerization conditions of constant temperature and constant monomer concentration. The activity usually exhibits a maximum followed by a rate decay to, more or less, a steady-state level of activity; however, more complicated activity profiles, for example, profiles with two maxima, have been reported by Han-Adebekun et al.[5] The specific shape of the activity profile depends on catalyst preparations and polymerization conditions.[6] The maximum rate could appear at the start of the polymerization or after a few hours; i.e., the acceleration period could be very short or quite long. The order of power-law rate functions with respect to monomer concentration for the overall polymerization rate may not be a constant and could be a noninteger ranging from less than unity to greater than unity with respect to olefin monomer concentration.[7,8] Kinetic behavior can also be affected by monomer diffusion in such a way that monomer concentration gradients would be established around active sites as a function of time and position. The establishment of monomer concentration gradients around active sites would affect the shape of polymerization rate profiles and the properties of the polymer formed.[9,10]

Very little research has been reported in the open literature on the effects of polymerization conditions (monomer concentration and reaction temperature) on the kinetics and product properties of polymers made with morphology-controlled Ziegler−Natta catalysts. In the current work, we report on the activity of Ziegler−Natta catalyst consisting of spherical $MgCl_2$ particles containing $TiCl_4$. The effect of operation conditions on activity profiles and product properties was investigated for a wide range of reaction temperature and ethylene concentrations.

Experimental Section

Materials. Anhydrous magnesium chloride (98%), ethyl alcohol (anhydrous, denatured), anhydrous heptane (99%), anhydrous hexanes, titanium tetrachloride (99.9%), and neat triethylaluminum (93%) were obtained from Aldrich and used without further purification. Vaseline and dibutyl phthalate (>98%) were obtained from Fluka and used without further purification. Sodium chloride with an average particle size of about 0.5 mm and 1,2,4-trichlorobenzene (HPLC grade) were obtained from Fisher Scientific. Polymer-grade ethylene was obtained from Matheson. Prepurified nitrogen and ultrahigh-purity hydrogen were obtained from Praxair. Ethylene, nitro-

10.1021/ma990841u CCC: $18.00 © 1999 American Chemical Society
Published on Web 11/10/1999

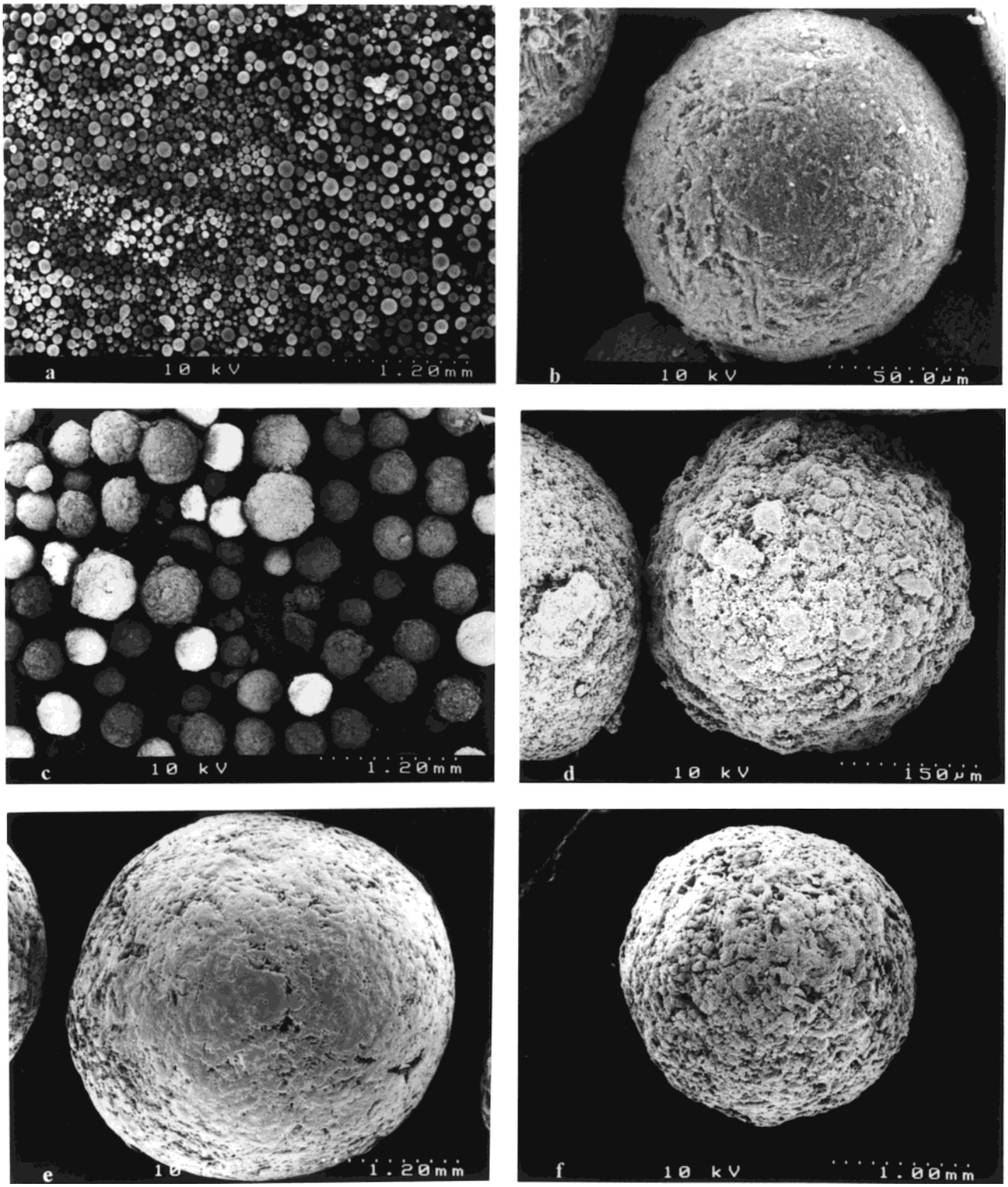

Figure 1. SEM micrographs of catalyst particles (a and b), prepolymer particles (c and d), and polymer granules (e and f).

gen, and hydrogen were each passed through a series of Alltech high-pressure gas purifiers containing BASF R3-11 catalyst, Ascarite, and 3A molecular sieves for the removal of oxygen, carbon dioxide, and moisture, respectively. Complete details of the feed purification, monitoring, and control equipment were previously described by Lynch and Wanke.[11]

Preparation of Catalyst. The morphology-controlled $MgCl_2$-supported $TiCl_4$ Ziegler−Natta catalyst was prepared in our laboratory by a method similar to that described by Ferraris et al.[12] No information on the preparation technique, other than the patent literature, could be found; hence, a detailed procedure is presented below. The general preparation procedure consisted of two steps. The first step was to prepare spherical $MgCl_2$ support by melt quenching of a $MgCl_2$−ethanol complex, and the second step consisted of treating the $MgCl_2$ support with $TiCl_4$ and an electron donor to obtain a very active, spherical catalyst.

The specific steps of melt quenching consisted of charging 220 g of Vaseline, 20 g of $MgCl_2$, and 40 mL of ethanol into a 1 L jacketed Pyrex vessel (from Büchi) equipped with a Rushton turbine stirrer and an exit port. The exit port of the 1 L vessel was connected through a valve to a Teflon tubing

with an inside diameter of 1.5 mm and a length of about 3 m. The other end of the Teflon tubing was dipped into a 3 L vessel containing 1 L of heptane, which was cooled to about −30 °C by an ethylene glycol−water mixture. In the 1 L vessel, an emulsion of $MgCl_2$−ethanol complex in Vaseline was formed at 120 °C by stirring at 1000 rpm. The emulsion was then forced out of the 1 L vessel by pressurizing it with nitrogen to 600 kPa. The emulsion flowed through the small diameter Teflon tubing and then into the cold heptane where it solidified rapidly. After the Vaseline was washed away with heptane, the powder of the $MgCl_2$−ethanol complex was transferred into a glass tube, having a fritted disk at the bottom, for a thermal treatment. The thermal treatment partially dealcoholated the $MgCl_2$−ethanol complex. The temperature for the thermal treatment increased steadily from room temperature to 120 °C in 4 h. After the thermal treatment, about 50% of ethanol was eliminated, and the molar ratio of ethanol to $MgCl_2$ was about 1.5 in the partially dealcoholated $MgCl_2$−ethanol complex.

The second step of the preparation of the catalyst consisted of treating the partially dealcoholated $MgCl_2$−ethanol complex with $TiCl_4$ and an electron donor. Special precautions, such as operating environment and purity of other chemicals used, are required for handling toxic and air-sensitive chemicals such as $TiCl_4$. About 5 g of the partially dealcoholated $MgCl_2$−ethanol complex, suspended in 150 mL of heptane, was introduced into a 500 mL glass flask equipped with a mechanical agitator. About 150 mL of $TiCl_4$ was added into the flask slowly to remove ethanol in the $MgCl_2$−ethanol complex by reaction with $TiCl_4$ and to fix additional $TiCl_4$ on the $MgCl_2$ support. The temperature of the flask was increased slowly from −20 to 50 °C in about 7 h while stirring slowly at 15 rpm. It is crucial that the stirring be gentle; rapid stirring results in breakup of the $MgCl_2$−ethanol particles. When the temperature reached 50 °C, about 0.6 mL of dibutyl phthalate, an electron donor, was added into the flask. The mixture was then heated to 110 °C in 3 h and kept at 110 °C for 1 h. After the liquid was removed, an additional 150 mL of $TiCl_4$ was added into the flask, and the temperature was kept at 110 °C for another 1 h. The reaction product in the flask was then cooled to 50 °C and washed with 100 mL of heptane. The wash was repeated 10 times; hexane was used for the last wash. The particles thus obtained were dried in a vacuum at room temperature for 30 min. The dry solid catalyst contained 3.7 wt % Ti as determined by a colorimetric analysis method.[13] Examination of the catalyst particles with scanning electron microscopy (SEM) showed that the dry solid catalysts were mostly in spherical form; sample micrographs are shown in Figure 1a,b.

Preparation of Prepolymerized Catalyst. A 1 L jacketed Pyrex reactor was used for the prepolymerization of ethylene in a semibatch reactor system operated in a slurry mode. The data acquisition system was previously described by Lynch and Wanke.[11] The $TiCl_4/MgCl_2$ catalyst prepared by the above procedure was exposed to mild polymerization condition in the semibatch reactor containing 300 mL of heptane in which the catalyst and polymer were suspended. Neat triethylaluminum of 0.25 mL as cocatalyst and 100 mg of catalyst were injected into the reactor. The prepolymerization was carried out at 30 °C in the presence of hydrogen pressure of 86 kPa and ethylene pressure of 62 kPa for about 3 h. After the prepolymerization, prepolymer particles were dried in a vacuum at room temperature for 30 min; about 7.3 g of polyethylene prepolymer, i.e., prepolymerized catalyst, was obtained. SEM micrographs of prepolymerized catalyst particles are shown in Figure 1c,d.

Ethylene Homopolymerization Experiments. A stainless steel semibatch reactor system, which was previously described,[11] was used for gas-phase polymerization at various reaction conditions, such as temperatures, hydrogen pressure, and ethylene pressure. For all the gas-phase runs except one, the reactor was charged with sodium chloride as a seedbed, neat triethylaluminum as a cocatalyst, and prepolymerized catalyst. (Rulon LR particles were used as the seedbed in one run; Rulon LR is the trademark of the Furon Co. for a very stable engineered polymer consisting mostly of poly(tetrafluoroethylene).) Polymerization temperature inside the reactor was kept constant by adjusting the temperature of the oil bath surrounding the reactor. Three types of operating procedures were used, i.e., type A, B, and C. For both type A and B operations, the reactor pressure was kept constant throughout the run. For type A operations, a desired amount of hydrogen was fed to the reactor at the beginning of the experiment followed by continuous addition of ethylene; ethylene was fed at a rate that kept the pressure constant at the desired set value. Type B operation was similar to type A except that no hydrogen was fed to the reactor. Type A and B experiments were done to define the dependencies of the activity profiles and polymer properties on operating conditions.

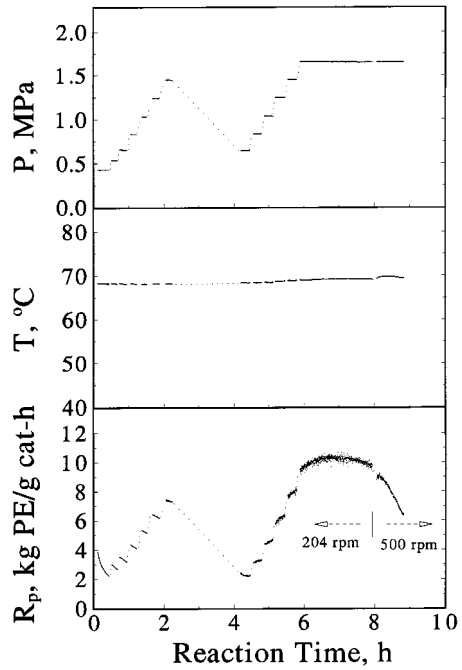

Figure 2. Pressure, temperature, and polymerization rate of a typical type C experiment.

Type C experiments were also carried out in the absence of hydrogen, but the ethylene pressure was varied during a given experiment. Stepwise increases in ethylene pressure were followed by a period of no ethylene feed (reactor pressure decreased); then, another set of step increases in ethylene pressures followed. Typical ethylene pressure changes and corresponding polymerization rates as a function of time for type C operation are illustrated in Figure 2. Type C experiments were done in an attempt to separate polymerization kinetics from activation−deactivation kinetics.

For all runs, ethylene feed rates were monitored by Matheson mass flow transducers, and the values of the flow rate, temperatures, and reactor pressure were recorded as a function of time at 10 s intervals by a data acquisition system.[11] Polymerization conditions, for type A, B, and C experiments, are summarized in Table 1. Typical SEM micrographs of polymer granules are shown in Figure 1e,f (polymer granules shown in Figure 1e,f are from run A2).

Measurement of Molar Masses. The molar masses of polyethylene were measured by size exclusion chromatography (SEC) with a Waters 150C GPC equipped with a differential refractometer and a series of four Shodex GPC/UT-800M columns. The columns and the detector were maintained at 140 °C; the solvent, HPLC grade 1,2,4-trichlorobenzene (from Fisher), was pumped through the columns at 1.0 cm^3/min. The 1,2,4-trichlorobenzene contained approximately 0.25 g/L of 2,6-*tert*-butyl-4-methylphenol as an antioxidant. Polyethylene concentrations of 0.035 to 0.07 mass % in 1,2,4-trichlorobenzene were injected into the SEC. Polystyrene samples of known molar masses (from TSK Standards), linear paraffins (C_{20}, C_{40}, and C_{60} from Fluka), and polyethylene reference materials

Table 1. Run Conditions[a] for Gas-Phase Polymerization of Ethylene

run type	run no.	amount of TEAL (mL)	amount of prepolymerized catalyst (mg)	T (°C)	hydrogen press. (MPa)	range of ethylene press. (MPa)	time (h)
A	A1	0.25	45	68.1	0.36	1.39	2.0
	A2[b]	0.25	200	70.5	0.31	1.37	2.0
	A3	0.25	63	67.9	0.35	0.69	2.0
B	B1	0.30	95	30.1	0	0.68	8.1
	B2	0.30	30	41.9	0	0.68	8.2
	B3	0.30	85	50.1	0	0.67	8.2
	B4	0.30	88	59.9	0	0.68	8.1
	B5	0.30	63	68.7	0	0.67	8.1
C	C1-a	0.30	94	31.5	0	0.38−1.59	
	C1-b			31.3		0.86−1.99	
	C2-a	0.30	108	29.9	0	0.35−1.77	
	C2-b			30.2		0.97−1.98	
	C3-a	0.30	103	39.2	0	0.53−1.39	
	C3-b			39.6		0.55−1.37	
	C4-a	0.30	90	40.2	0	0.34−1.55	
	C4-b			40.6		0.55−1.55	
	C5-a	0.30	95	49.8	0	0.35−1.36	
	C5-b			50.2		0.37−1.35	
	C6-a	0.30	84	50.0	0	0.34−1.35	
	C6-b			50.4		0.39−1.35	
	C7-a	0.30	96	59.5	0	0.35−1.35	
	C7-b			60.2		0.36−1.36	
	C8-a	0.30	90	59.8	0	0.33−1.35	
	C8-b			60.1		0.34−1.35	
	C9-a[c]	0.35	80	69.3	0	0.34−1.27	
	C9-b			69.6		0.54−1.28	
	C10-a	0.30	94	68.4	0	0.34−1.36	
	C10-b			68.7		0.55−1.56	

[a] The stirring speed of the reactor was 204 rpm, and the seed bed was 100 g of NaCl used for all the runs unless specified. [b] The seed bed for this run was 35 g of Rulon LR particles (about 2 × 2 × 2 mm by length). [c] The seed bed for this run was 200 g of NaCl.

Table 2. Effect of the Amount of the Prepolymerized Catalyst on the Yield of Gas-Phase Ethylene Homopolymerization[a]

run no.	seed bed	prepolymerized catalyst (mg)	P_{H_2} (MPa)	$P_{C_2H_4}$ (MPa)	T (°C)	yield (g of PE/g of cat. h)	bulk density (g/cm^3)
A1	NaCl 100 g	45	0.36	1.39	68.1	4589	0.45
A2	Rulon 35 g	200	0.31	1.37	70.5	4957	0.45
A3	NaCl 100 g	63	0.35	0.69	67.9	1193	0.42

[a] See Table 1 for other polymerization conditions.

1475, 1482, 1483, and 1484 (from NIST) were used as standards for the molar mass calibrations.

Results and Discussion

Mass Transfer and Heat Transfer Effects. Mass transfer resistances of monomer in the growing polymer particles were predicted to affect polymerization rate profiles as well as polymer properties due to the monomer concentration gradients established across polymer particles.[10] A well-defined transport resistance model, the multigrain model, described that mass transfer can occur at microparticle and macroparticle levels and at the particle external boundary layer.[9,10] This model predicts that reaction temperature, monomer pressure, and catalyst particle size affect mass transfer resistance of monomer during polymerization. Increase in catalyst particle size and reaction temperature and decreases in monomer pressure are predicted to increase mass transfer resistance. As mass transfer resistance increases, the initial maximum polymerization rate will appear at later times for catalyst with activity profiles that show an initial increase followed by a decrease in activity. The molar masses of the polymer produced will decrease, and its polydispersity will increase as mass transfer resistance increases. The heat transfer effects, predicted by the multigrain model, can be significant with increasing catalyst particle sizes.

In the current study, the effect of external mass transfer and heat transfer from the reactor was examined by changing the amount of prepolymerized catalyst and the stirring speed in the polymerization. Table 2 shows the polymerization yield at different amounts of prepolymerized catalyst and different seed beds and bulk densities of polyethylene made (runs A1, A2, and A3 in Table 1). The temperature in the reactor was well controlled for all the type A experiments. As seen in Table 2, the yield does not change with changes in the amount of prepolymerized catalysts from 45 to 200 mg. Changing stirring speed from 204 to 500 rpm did not increase the polymerization rate (seen in Figure 2). Therefore, it can be concluded that external mass transfer and heat transfer resistances are negligible during polymerization at the above conditions.

Using morphology-controlled catalyst, the properties of polyethylene, such as molar masses, can be measured as a function of polymer granule size. In a single polymerization run, larger catalyst particles should grow to larger polymer granules if all the catalyst particles have equal specific activity; i.e., the rate of polymerization per unit mass of catalyst is independent of catalyst particle size. Large polymer granules are more likely subjected to internal mass transfer resistances during polymerization than the small particles, especially under polymerization conditions of high temperature and low ethylene pressure. Mass transfer

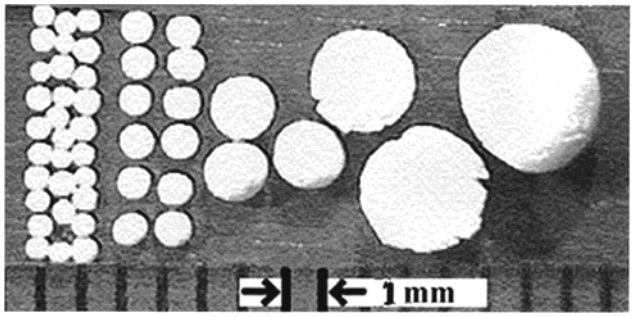

Figure 3. Optical micrograph of different sizes of polyethylene granules used for molar masses measurement (from run A3 of Table 1).

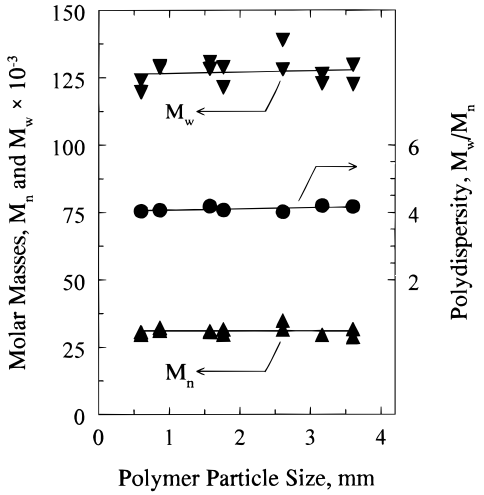

Figure 4. Dependence of number-average molar mass (M_n), weight-average molar mass (M_w), and polydispersity on the size of polyethylene granules.

resistances should result in polymer with lower molar masses and wider molar mass distribution.

Large polymer granules are also more likely subjected to internal heat transfer resistances during polymerization than the small particles.[9] Under the effects of heat transfer resistances, the temperature of large particles will be higher than that of small particles. Jejelowo et al. studied the effect of polymerization temperature on the molar masses and polydispersity of polyethylene produced in the gas-phase with deactivation polymerization rate profiles; they found that increases in temperature caused unequivocally decreases in the molar masses and increases in polydispersity.[14]

In this study, the polyethylene molar masses were measured as a function of polyethylene granule size. The polymer granules from a single run (run A3 in Table 1) were manually sorted into seven sets of sizes as shown in Figure 3. Hydrogen was added into the reactor to lower molar masses of polyethylene and make the SEC measurement of molar masses more reliable. The dependencies of number-average molar mass (M_n), weight-average molar mass (M_w), and polydispersity of polyethylene on the sizes of polyethylene granules shown in Figure 3 are plotted in Figure 4. Each sample was measured twice as indicated by solid symbols, and the lines are linear regression lines. The results in Figure 4 show that molar masses and polydispersity are not a function of polymer granule sizes; this implies that mass transfer and heat transfer resistances were not significantly present under the experimental conditions used. Thus, it can be inferred that there were negligible effects

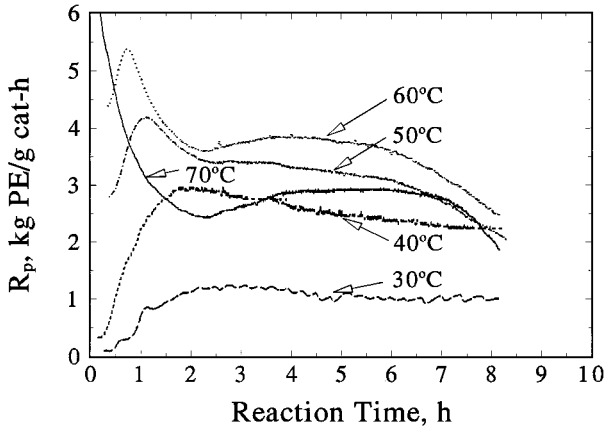

Figure 5. Polymerization rate profiles as a function of polymerization temperature at ethylene pressure of 680 kPa.

of mass transfer and heat transfer in ethylene polymerization using the prepolymerized catalyst at any ethylene pressure above 0.69 MPa and at any polymerization temperature below 70 °C. The observation that M_w and M_n values were independent of polymer particle size also supports the assumption that the size distribution of the polymer particles resulted from the size distribution of the catalyst particles, i.e., constant specific activity so that large catalyst particles produced large polymer particles and small catalyst particles produced small polymer particles. If the kinetic behavior depended on catalyst particle size, e.g., small catalyst particles resulting in large polymer particles, then the lack of variation of M_w and M_n with polyethylene granule size would be very unlikely.

Polymerization Rate Profiles. The polymerization rate profiles at a constant ethylene pressure, as a function of polymerization temperature, are shown in Figure 5 (runs B1 to B5). No hydrogen was used to simply the procedure and increase the reproducibility of experiments. In each run, ethylene pressure and polymerization temperature were controlled at constant levels. The polymerization rate was calculated from the rate of ethylene addition to the reactor. No agglomeration of polymer particles was observed even after 8 h of reaction time, but most of the polymer granules are broken into smaller pieces after 8 h due to the grinding by the salt seed bed and attrition by stirrer blades.

The following observations can be made from the results of type B experiment presented in Figure 5:

1. All the activity profiles show deactivation at longer times.

2. For low reaction temperatures (≤40 °C), there is a single maximum in the activity profiles.

3. For higher reaction temperatures (≥50 °C), the activity profiles have two maxima (the two maxima will be referred to as the first peak and the second peak, respectively).

4. The first peaks shift from longer to shorter times, and the second peaks become more pronounced with increasing polymerization temperature.

5. The second peaks are broader than the first peaks, and the second peak would not be observed if the polymerization is less than 2 h.

6. The overall polymerization rate increases with increasing temperature up to 60 °C and then decreases at higher temperature.

At low polymerization temperatures, the rate profiles show a hybrid-type activity profile with an initial

accelerating period followed by deactivation. According to simulation results of the multigrain model, the hybrid-type rate profile is the first telltale sign of the existence of mass transfer resistance, and if mass transfer is controlling, the first maximum in the rate will shift to the right-hand side (longer time) with increasing temperature.[10] This is not the case seen in Figure 5, which shows that the first peaks shift to the left-hand side (shorter time) with increasing polymerization temperature. Such an observation provides an additional evidence that mass transfer resistances are negligible in the gas-phase ethylene polymerization system at the experimental conditions used.

The shift of the first maximum from longer to shorter times in the polymerization rate profiles with increasing temperature can be explained by the existence of an initiation step of catalytic sites by ethylene before chain propagation. If the initiation rate is sensitive to temperature, the initiation rate constant would increase with the increase of polymerization temperature. At low temperature, the low initiation rate constant would give a long accelerating period. At high temperature, the accelerating period would be shorter.

The appearance of the second peaks implies the presence of the second type of catalytic sites in this prepolymerized catalyst (site 1 for the first peaks and site 2 for the second peaks). The nature of these sites is not known, but it is unlikely that the different sites are due to Ti in different oxidation states since Chien et al. reported that the distribution of oxidation states of various active Ti does not change with time after 30 min of polymerization.[15] As shown in Figure 5, the second peaks appear much later than 30 min; hence, the change of oxidation states of Ti during polymerization was probably not the reason for the appearance of the second peaks.

The observation on the relative broadness of the first and second peaks in Figure 5 has not been reported in the literature. A quantitative model is needed to determine whether the relative broadness of the first and second peaks is related to the activation and deactivation steps for site 1 and site 2 in the polymerization. We are currently trying to develop such a quantitative model for the activity profiles shown in Figure 5.

The temperature effect on the polymerization rate in Figure 5 also shows that the overall polymerization rate increases with increasing temperature up to 60 °C and then decreases at higher temperature. Similar temperature effects over a range of 30−70 °C were observed by Dusseault and Hsu with a maximum in productivity at 55 °C for gas-phase polymerization of ethylene using $MgCl_2$/ethyl benzoate/$TiCl_4$ + triethylaluminum catalyst at high Al/Ti ratio.[16] An Arrhenius plot of the experimental results in Figure 5 is shown in Figure 6 by the solid circles and a solid line. In Figure 6, the polymerization rate, R_p, is the average rate over the 8 h of each run; the ethylene concentration, [M], is the gas-phase concentration in the reactor calculated using the Peng−Robinson equation of state[17] following the method by Bu et al.[8] It is seen in Figure 6 that the rate normalized with respect to [M] is not linear, but it has a maximum at 60 °C. The appearance of a maximum in the rate has been explained by the deactivation of catalytic sites at higher temperatures or by the sorption theory.[18] In the sorption theory, the polymerization rate is assumed to be proportional to the monomer concentration in the amorphous polymer around the surface of catalytic sites, not the bulk monomer concentration in the reactor. With increasing temperature, the extent of sorption decreases, causing a decrease in the rate of polymerization. The concentration of sorbed ethylene can be expressed by Henry's law according to eq 1:

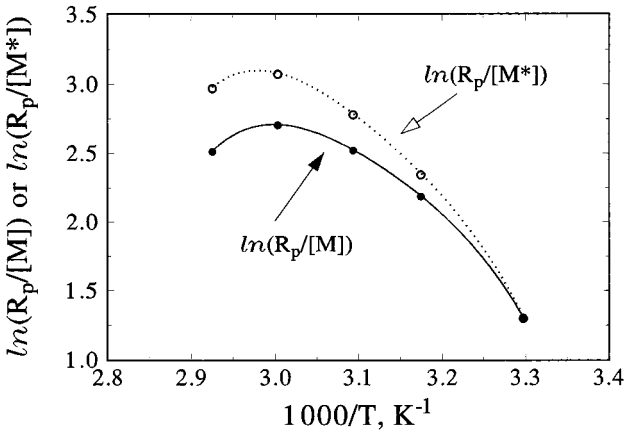

Figure 6. Arrhenius plot of the average polymerization rate.

$$[M^*] = k_H P \quad (1)$$

where [M*] is the ethylene concentration in the amorphous polymer, k_H is a Henry's law constant, and P is the monomer pressure in the reactor. The temperature effect on the Henry's law constant, k_H, for the sorption of ethylene in the polyethylene, has been correlated by Stern et al. to the following equation:[19]

$$\log(k_H) = -2.38 + 1.08(T_c/T)^2 \quad (2)$$

where T_c is the critical temperature of ethylene. The Arrhenius plot, based on eq 1 using relative ethylene concentration sorbed in polyethylene predicted by eq 2 and normalized to 30 °C, is also shown in Figure 6 by the open circles and a dotted line. It is seen in Figure 6 that sorption effects alone do not remove the maximum in the average polymerization rate as a function of temperature. Therefore, the low polymerization rate at high temperatures was mainly caused by catalyst deactivation. The shapes of the activity profiles and relative temperature dependence of rate on temperature at higher ethylene pressure (up to 2 MPa) were similar to those shown in Figures 5 and 6.

Power-Law Order with Respect to Ethylene Concentration in Power-Law Rate Function. Fitting the overall rate of polymerization R_p on ethylene concentration [M] at a constant temperature for Ziegler−Natta ethylene homopolymerization by a power-law rate function has yielded a range of power-law orders with respect to ethylene concentration. For a SiO_2/$MgCl_2$ supported $TiCl_4$ catalyst with constant polymerization rate, power-law orders have been reported from less than unity to 1.5 at temperature range of 30−70 °C by Bu et al.[8] and from 1.5 to 1.6 at temperature range of 80−90 °C by Kissin.[7]

Kinetic analysis of most ethylene polymerization is complicated by catalyst deactivation and the possible presence of mass and heat transfer effects. We have shown above that mass transfer and heat transfer effects were not significant in the current study. Hence, the rates of polymerization measured in this study are intrinsic rates; however, the concentration of active sites, [C*], is a function of time due to catalyst activa-

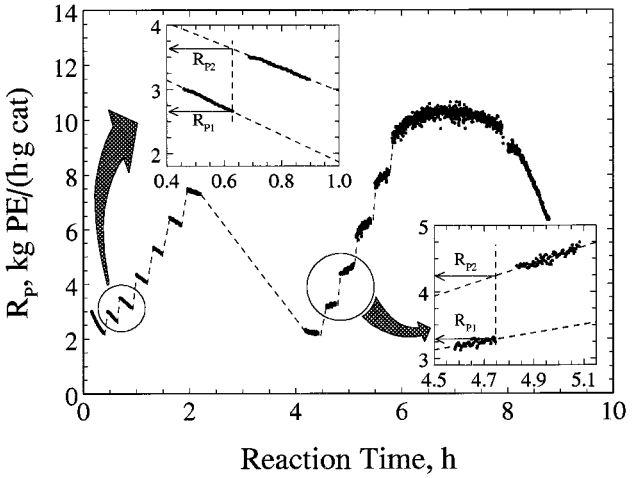

Figure 7. Illustration of obtaining $R_{p1}(t_i)$ and $R_{p2}(t_i)$ at a specific time t_i for eq 6 with the change of ethylene pressure by extrapolation of polymerization rate profile in a typical type C experiment.

tion−deactivation. A simple power-law rate expression, as a function of ethylene concentration ([M]) and active site concentration ([C*]), for this case is given by eq 3

$$R_p = k[M]^n[C^*(t)] \tag{3}$$

The usual method of estimating values of the power-law order n for deactivating systems is to decouple the polymerization kinetics from the deactivation kinetics by assuming a functional dependence for [C*][20] and then fitting the measured rates to the combined polymerization−deactivation model. At times a simple power-law rate function is used to fit polymerization rate data without separating polymerization and deactivation kinetics.[21] We have attempted to experimentally decouple the polymerization and deactivation kinetics by measuring the rates of polymerization at two different ethylene concentrations at approximately the same time. This was done by changing the ethylene pressure in the reactor rapidly (type C experiments) and then extrapolating the rate of polymerization at the new ethylene pressure to the time at which the pressure change was made. This procedure is illustrated in Figure 7.

Applying eq 3 at a time, t_i, at which the ethylene concentration was changed from $[M]_1$ to $[M]_2$, yields

$$R_{p1}(t_i) = k[M]_1^n[C^*(t_i)] \tag{4}$$

$$R_{p2}(t_i) = k[M]_2^n[C^*(t_i)] \tag{5}$$

Then, taking the ratio of eq 5 to eq 4 and solving for n yields

$$n = \frac{\ln(R_{p2}/R_{p1})}{\ln([M]_2/[M]_1)} \tag{6}$$

The power-law order, n, can be calculated directly from eq 6 without making any assumption about the activation−deactivation kinetics.

Values of the power-law orders, calculated according to eq 6, were a function of time-on-stream; values of n as a function of time-on-stream are shown in Figures 8−12 for reaction temperatures of 30, 40, 50, 60, and 69 °C. At every temperature, at least two runs were

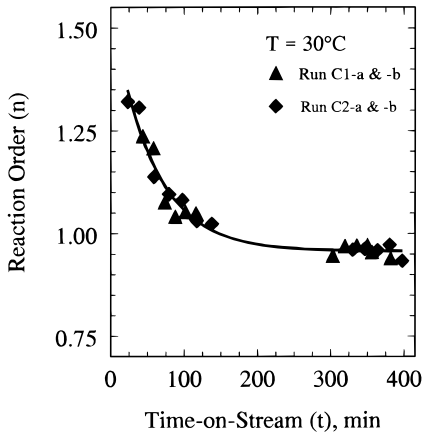

Figure 8. Dependence of power-law order n on time at polymerization temperature of 30 °C.

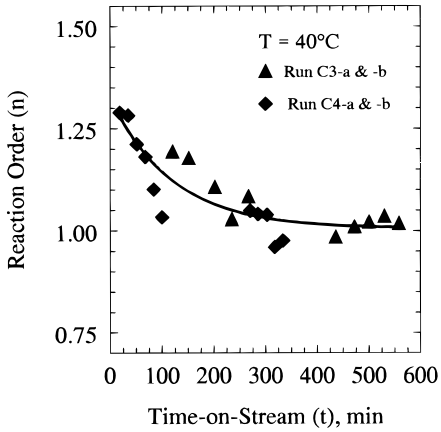

Figure 9. Dependence of power-law order n on time at polymerization temperature of 40 °C.

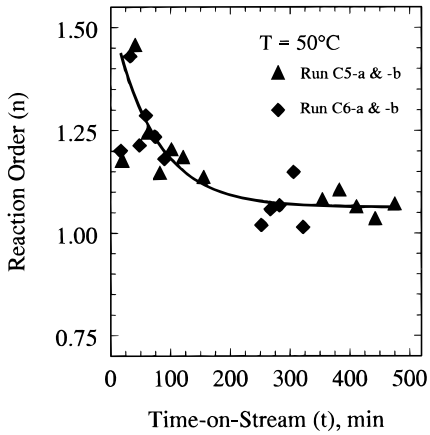

Figure 10. Dependence of power-law order n on time at polymerization temperature of 50 °C.

done as shown in Figures 8−12 by different symbols (runs C1 to C10, Table 1). The reproducibility for the repeat runs was very good. From Figures 8−12, it is clearly shown that the values of n, the power-law orders with respect to ethylene concentration, change with polymerization time, generally from about 1.5 for the first 2−3 h to a constant level after about 2−3 h of polymerization, regardless of the ethylene concentration. Values of the power-law order n obtained from Figures 8−12 are summarized in Table 3. It is seen from Table 3 that the constant values of n after 2−3 h of polymerization tend to be slightly less than unity at

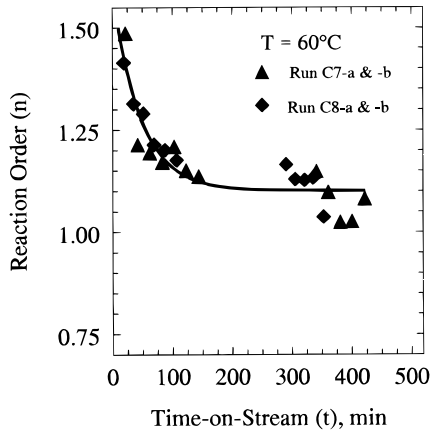

Figure 11. Dependence of power-law order *n* on time at polymerization temperature of 60 °C.

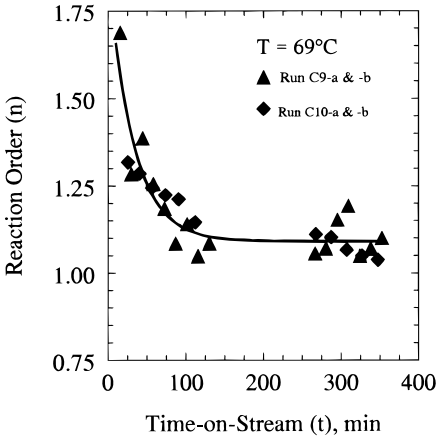

Figure 12. Dependence of power-law order *n* on time at polymerization temperature of 69 °C.

Table 3. Comparison of Power-Law Orders Obtained by Equations 6 and 7

		values of power-law orders			
		n (based on eq 6)		*n′* (based on eq 7)	
run no.[a]	temp, °C	0−2 h	4−7 h	0−2 h	4−7 h
C1	31.4	1.30−1.03	0.96	1.15	0.93
C2	30.0			1.17	0.87
C3	39.4	1.30−1.12	1.00	1.07	1.03
C4	40.3			1.24	1.05
C5	50.1	1.45−1.14	1.04	1.11	1.20
C6	50.2			1.21	1.21
C7	59.9	1.50−1.15	1.10	0.92	1.19
C8	60.0			0.95	1.22
C9	69.5	1.70−1.10	1.10	0.65	1.10
C10	68.6			0.86	1.38

[a] The complete run conditions are listed in Table 1.

lower temperatures and slightly above unity at higher temperatures.

The above method of obtaining apparent orders of reaction with respect to monomer concentration results in significantly different reaction orders than those obtained by direct fitting of rate data by a power-law rate function that ignores the changes in active site concentration, i.e.,

$$R_p = k'[M]^{n'} \tag{7}$$

where k' includes the active site concentration. Apparent orders obtained from eqs 6 and 7 are compared in Table 3. [Note: the same rate data were used to estimate the values of *n*.] It is not surprising that the values of n' obtained from eq 7 are different from values of *n* obtained from eq 6 since k' is not constant for systems with time varying activities. The fits of the data for all the runs (C1 to C10) by eq 7 were very good if the data for each run were split into short time-on-stream (0 to about 2 h) and long time-on-stream (typically 4−7 h) regions. The short and long time-on-stream regions can be readily identified in Figures 8−12. All correlation coefficients were ≥0.982. (The average r^2 value for all 20 fits was 0.996.) A typical fit of the data by eq 7 is shown in Figure 13.

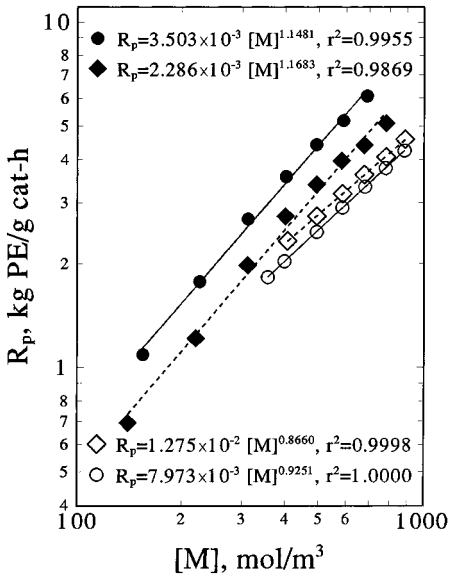

Figure 13. A log−log plot of ethylene concentration versus polymerization rate by eq 7 for runs C1 (solid regression lines) and C2 (dash regression lines) at the beginning of run (solid symbols) and the end of run (open symbols).

It is surprising that the data for time-varying activities are so well correlated by eq 7 which ignores the time dependence of the active site concentration; Han-Adebekun and Ray also found that eq 7 provided a good correlation for both ethylene and propylene polymerization rate over a deactivating catalyst.[21] However, the values of n' obtained from eq 7 do not provide information on the kinetics of the polymerization (propagation) step, i.e., the monomer dependence of the specific polymerization rate since the n' depend heavily on whether the data used to obtain the value of n' are measured at a time when the activity of the catalysts is increasing or decreasing. During periods of increasing rate, the n' values from eq 7 are higher than the "true" power-law orders, and during periods of decreasing rates (catalyst deactivation), the values of n' are lower than the "true" power-law orders. This dependence on the shape of the activity profiles of the apparent order determined using eq 7 is evident in the temperature dependence of n' shown in Table 3. At temperatures of 30 and 40 °C and low reaction times, the activity of the catalysts increased; this resulted in high values of n' (see activity profiles in Figure 5). At temperatures of 50 and 60 °C and low reaction times, the activity of the catalysts first increased and then decreased; this resulted in intermediate values of n'. At 70 °C and low reaction times, the activity of the catalysts decreased; this resulted in low values of n'. The changes in catalytic activities for longer times-on-stream are also reflected in the trend in the n' values; e.g., at higher reaction

temperatures (60 and 70 °C), the n' values are higher because the catalytic activity was increasing.

The n values obtained by the use of eq 6 should reflect the intrinsic kinetics of the polymerization process in the absences of activation−deactivation phenomena. The results in Table 3 indicate that the order with respect to ethylene at the beginning of the polymerization was 1.3−1.7, with higher values at higher reaction temperature. The order decreased to 0.96−1.1 for longer times-on-stream; again higher values were observed for higher temperatures.

This time dependence of n, just like the previously discussed activity profiles, indicates the presence of at least two catalytic sites which have different activation, propagation and deactivation kinetics. If it is assumed that the catalyst contains two distinctly different sites, site 1 and site 2, then the variation of n with time and temperature provides information, in addition to that inferred form the activity profiles, about the behavior of the catalytic sites. The order of the overall dependence of polymerization rate with respect to ethylene concentration for site 1, which has more rapid activation and deactivation than site 2, varies between one and two while the order for site 2 appears to be close to unity. Site 1 appears to dominate the polymerization behavior during the initial stages of polymerization while site 2, which activates and deactivates slowly, appears to govern the behavior after several hours on stream. The values of n, determined by the new method (use of eq 6), do not provide information on the deactivation kinetics, but evidence of at least two types of deactivation behavior has been reported for gas-phase polymerization of ethylene by Dusseault and Hsu.[16] Various types of deactivation behaviors will be examined in the kinetic modeling of the experimental results reported in this study.

Conclusions

Examination of mass transfer effect, polymerization rate profiles, and power-law orders with respect to ethylene concentration provided details in some aspects for kinetic modeling of ethylene homopolymerization over laboratory-made, morphology-controlled, prepolymerized $MgCl_2$-supported $TiCl_4$ catalyst. Mass transfer effects were negligible at the ethylene polymerization conditions used. Polymerization rate profiles changed dramatically with time and showed two maxima in the rates; these were especially pronounced at high polymerization temperatures. A new method for determining power-law orders for systems with time-varying catalytic activities was proposed. Power-law orders, using this new method, with respect to ethylene concentration were not constant; the dependence of the change of the power-law orders with polymerization time and temperature provided insight into the polymerization kinetics. These results show that at least two different types of catalytic sites are present in the heterogeneous $MgCl_2$−$TiCl_4$ Ziegler−Natta catalyst and suggest these catalytic sites have different rate functions and activation−deactivation behaviors.

Acknowledgment. The support of this work by the Natural Sciences and Engineering Research Council of Canada and NOVA Chemicals Corporation is gratefully acknowledged. We thank N. Bu for measuring the molar masses and C. Barker for performing the SEM work.

References and Notes

(1) Boor, J., Jr. In *Ziegler−Natta Catalysts and Polymerization*; Academic Press: New York, 1979.
(2) Galli, P.; Haylock, J. C. *Prog. Polym. Sci.* **1991**, *16*, 443.
(3) Di Drusco, G.; Rinaldi, R. *Hydrocarbon Process.* **1984**, *11*, 113.
(4) Covezzi, M. *Macromol. Symp.* **1995**, *89*, 577.
(5) Han-Adebekun, G. C.; Hamba, M.; Ray, W. H. *J. Polym. Sci., Part A: Polym. Chem.* **1997**, *35*, 2063.
(6) Kissin, Y. V. In *Isospecific Polymerization of Olefins with Heterogeneous Ziegler−Natta Catalysts*; Springer-Verlag: New York, 1985.
(7) Kissin, Y. V. *J. Mol. Catal.* **1989**, *56*, 220.
(8) Bu, N.; Lynch, D. T.; Wanke, S. E. *Polym. React. Eng.* **1995**, *3* (1), 1.
(9) Floyd, S.; Choi, K. Y.; Taylor, T. W.; Ray, W. H. *J. Appl. Polym. Sci.* **1986**, *31*, 2231.
(10) Floyd, S.; Heiskanen, T.; Taylor, T. W.; Mann, G. E.; Ray, W. H. *J. Appl. Polym. Sci.* **1987**, *33*, 1021.
(11) Lynch, D. T.; Wanke, S. E. *Can. J. Chem. Eng.* **1991**, *69* (2), 332.
(12) Ferraris, M.; Rosati, F.; Parodi, S.; Giannetti, E.; Motroni, G.; Albizzati, E. US Patent 4,399,054, 1983.
(13) Vogel, A. I. In *A Text-Book of Quantitative Inorganic Analysis Including Elementary Instrumental Analysis*, 3rd ed.; Longmans: London, 1961.
(14) Jejelowo, M. O.; Lynch, D. T.; Wanke, S. E. *Macromolecules* **1991**, *24*, 1755.
(15) Chien, C. W. C.; Weber, S.; Hu, Y. *J. Polym. Sci., Part A: Polym. Chem.* **1989**, *27*, 1499.
(16) Dusseault, J. J. A.; Hsu, C. C. *J. Appl. Polym. Sci.* **1993**, *50*, 431.
(17) Peng, D.-Y.; Robinson, D. B. *Ind. Eng. Chem. Fundam.* **1976**, *15*, 59.
(18) Hutchinson, R. A.; Ray, W. H. *J. Appl. Polym. Sci.* **1990**, *41*, 51.
(19) Stern, S. A.; Mullhaupt, J. T.; Gareis, P. J. *AIChE J.* **1969**, *15*, 64.
(20) Doi, Y.; Murata, M.; Yano, K.; Keii, T. *Ind. Eng. Chem. Prod. Res. Dev.* **1982**, *21*, 580.
(21) Han-Adebekun, G. C.; Ray, W. H. *J. Appl. Polym. Sci.* **1997**, *65*, 1037.

MA990841U